Carbon and oxygen minibeam radiation therapy: an experimental dosimetric evaluation

Immaculada Martínez-Rovira[1,2],* Wilfredo González[1], Stephan Brons[3], and Yolanda Prezado[1]

[1] *Laboratoire d'Imagerie et Modélisation en Neurobiologie et Cancérologie (IMNC), Centre National de la Recherche Scientifique (CNRS). Campus universitaire, Bât. 440, 1er étage - 15 rue Georges Clemenceau - 91406 Orsay cedex (France)*

[2] *Ionizing Radiation Research Group (GRRI), Physics Department, Universitat Autònoma de Barcelona. Campus UAB, Avinguda de l'Eix Central, Edicifi C - 08193 Cerdanyola del Vallès (Barcelona, Spain) and*

[3] *Heidelberg University Clinic, Heidelberg Ion Beam Therapy Center (HIT), Im Neuenheimer Feld 672 - 69120 Heidelberg (Germany)*

This article has been accepted for publication and undergone full peer review but has not been through the copyediting, typesetting, pagination and proofreading process, which may lead to differences between this version and the Version of Record. Please cite this article as doi: 10.1002/mp.12383

Abstract

Purpose: To perform dosimetric characterization of a minibeam collimator in both carbon and oxygen ion beams to guide optimal set up geometry and irradiation for future radiobiological studies using these beams.

Methods: Carbon and oxygen minibeams were generated using a prototype tungsten multislit collimator presenting line apertures 700 μm wide, which are spaced 3500 μm centre-to-centre distance apart. Several radiation beam spots generated the desired field size of 15×15 mm^2 and production of a 50 mm long spread out Bragg peak (SOBP) centered at 80 mm-depth in water. Dose evaluations were performed with two different detectors: a PTW microDiamond® single crystal diamond detector and radiochromic films (EBT3). Peak-to-valley dose ratio (PVDR) values, output factors (OF), penumbras and full width at half maximum (FWHM) were measured.

Results: Measured lateral dose profiles exhibited spatial fractionation of dose at depth in a water phantom in the expected form of peaks and valleys for both carbon and oxygen radiation fields. The diamond detector and radiochromic film provided measurements of PVDR in good agreement. PVDR values at shallow depth were about 60 and decreased to about 10 at 80 mm-depth in water. OF in the center of the SOBP was about 0.4; this value is larger than the corresponding one in proton minibeam radiation therapy measured using comparable collimator due to a reduced lateral scattering for carbon and oxygen minibeams.

Conclusions: Carbon and oxygen minibeams may be produced by a mechanical collimator. PVDR values and output factors measured in this first study of these minibeam radiation types indicate there is potential for their therapeutic use. Optimization of minibeam collimator design and the number and size of focal spots for irradiation are advocated to improve PDVR values and dose distributions for each specific applied use.

Keywords: hadron therapy, minibeam radiation therapy (MBRT), carbon and oxygen beams

*Electronic address: immamartinez@gmail.com

I. INTRODUCTION

The unique physical and biological properties of charged particles provide a higher tumor dose conformability and an increased relative biological effectiveness (RBE) with respect to conventional radiotherapy (RT) [1–3]. Profiting from these advantages, hadron therapy (HT) has been successfully employed over the past years [4–7]. Among the different types of ion species, carbon ions are considered to have optimal properties, in terms of superior physical and biological characteristics [8]. Heavier ions are disfavoured by higher damage in the entrance channel, despite beneficial properties such as high RBE and reduced scattering. However, the combination of the benefits of heavy ions and of minibeam radiation therapy (MBRT) may further increase its therapeutic index since spatial fractionation of dose has been reported to increase the tolerance of normal tissue to radiation [9–11]. This indicates a potential for hadron MBRT to increase the therapeutic ratio in application to radio-resistant tumors by combining the attributes of increased radiation tolerance of normal tissues in MBRT with hadron beam high relative biological effectiveness and improved target dose conformation [12]. In particular, oxygen might be a good candidate to efficiently overcome radio-resistance of hypoxic tumors [13]. For this purpose, carbon and oxygen MBRT were evaluated in this study.

The dose profiles of MBRT consist in a pattern of peaks and valleys, *i.e.*, with high doses along the beams paths (peak dose) and low doses (valley dose) in the spaces between them [14, 15]. The ratio between the peak and the valley doses (peak-to-valley dose ratio, PVDR) is an important dosimetric parameter in spatially fractionated techniques, since it plays an important role in the biological response. To spare normal tissues, high PVDRs and low valley doses are requested [16, 17]. Doses as high as 100 Gy in one fraction were well tolerated by normal rat brain (whole brain irradiation), when using synchrotron 600 μm wide minibeams, in comparison with 22 Gy delivered in standard irradiations [9–11].

The combination of the prominent advantages of hadrons and MBRT has been proposed in previous works. Prezado *et al.* [18] showed the favorable dose distributions of proton MBRT (pMBRT) with 700 μm wide proton beams. As a result, pMBRT has been recently implemented at a clinical center [19]. A first biological indication of the advantages of carbon MBRT was presented in the work of Dilmanian *et al.* [20]. One rabbit brain was irradiated with arrays of 130 MeV/nucleon carbon 300 μm wide beams at a research facility (Brookhaven National Laboratory). Target doses of 40 Gy were deposited in a single fraction and little damage was observed in the surrounding brain [20]. Despite the limitations of this work (poor statistics and short-term follow up), the results suggested that segmented thin carbon beams can be used to reduce the impact on the non-targeted tissues in carbon therapy. However, statistically significant studies with clinical beams, including long-term follow-up and a dose-escalation, are needed to confirm the clinical potential of this technique. That is why the main aim of this work was to implement hadron MBRT at a clinical center (Heidelberg Ion-Beam Therapy Center-HIT [21, 22], Germany) and to perform a first dosimetric evaluation to guide the forthcoming radiobiological experiments.

Dosimetry measurements in carbon and oxygen MBRT are particularly challenging due to the small field sizes used (less than 1 mm), and the variation of linear energy transfer (LET) as a function of depth. These constraints limit the choice of detectors. Therefore, the first objective of our work was to evaluate the suitability of the chosen systems for carbon and oxygen MBRT. To the best of our knowledge, this is the first reported experimental dosimetry study using heavy ions with such small field sizes. The beams were chosen to be 700 μm wide for two reasons:

- This beam size is large enough not to be vulnerable to beam smearing from cardiac pulsations [23], and, therefore, extremely high dose rates, such as those available at synchrotrons, are not needed.
- To be able to compare our data with previous works in x-rays MBRT and in pMBRT [19, 24].

In the first phase, the main targets will be neurological, *i.e.* tumors that can be stabilized against pulmonary and/or cardiac cycles. That is why our evaluation is focused on the human head as the main final target, and therefore, clinical relevant energies were employed (150–300 MeV/nucleon). This novel RT approach might allow a reduction in the side effects in normal tissues. The potential gain in therapeutic index could open the door to an efficient treatment of very radio-resistant tumors. It might also make charged particle therapy more amenable to administration in either a single dose fraction or in a very small number of fractions. Finally, hadron MBRT might also be of interest for radio-surgical interventions, such as the treatment of Arteriovenous Malformations (AVMs), where high doses are applied in one fraction.

II. MATERIALS AND METHODS

A. Irradiation configuration

Irradiations (carbon and oxygen beams) were carried out at the fixed horizontal beam experimental station available at HIT (Germany) [21, 22]. The main irradiation parameters are described in Table I. Spread Out Bragg Peak (SOPB) irradiations, 50 mm long and centered at 80 mm-depth, were performed. SOBP beam intensities and energies were computed using the experimental planning program TRiP [25, 26]. In order to cover a given irradiation field size, several hundreds of beam spots per energy slice were used. The spot size was between 3.8–7.0 mm; the step size was 1 mm both in the horizontal and vertical direction. The beam momentum spread was around 0.1–0.2%. Beam divergence was less than 1 mrad [27].

TABLE I: Main irradiation parameters used in carbon and oxygen MBRT experiments: the field size (*Field size*) and the step size used to create the whole irradiation field size (*Step size*); the range of full width at half maximum focus sizes (*FWHM Focus*); the range of energies to create an SOBP of 50 mm centered at 80 mm-depth in water (labelled as *Energies*) and the energy step size in millimeters (*Energy step size*).

	^{12}C	^{16}O
Field size (mm^2)	15×15	15×15
Step size (mm^2)	1×1	1×1
FWHM Focus (mm)	4.6–7.0	3.8–4.9
Energies (MeV/nucleon)	165–230	196–272
Energy step size (mm)	3 (17 energies)	

Carbon and oxygen minibeam patterns were generated by interposing a first prototype of multislit collimator (MSLC) into the beam. The collimator is made of tungsten and was manufactured by electro-erosion (see Figure 1). This collimator was inspired by the one used in our previous work in proton MBRT [19]. It was designed with the same intended future research/clinical motivation: the treatment of radio-resistant brain tumors. The MLSC has several (5) 700 μm wide line apertures (beam width), separated by 3500 μm (center-to-center or c-t-c distance). The thickness, height and lateral dimensions of the MSLC are 70 mm, 90 mm and 20 mm, respectively. The latter dimension imposed an irradiated area of 15×15 mm^2, which would be enough to irradiate a whole rat brain in preclinical studies with neurological tumors as a first target. The distance between the collimator exit and the phantom entrance was 50 mm. A set of lasers present in the experimental room was used to align the collimator.

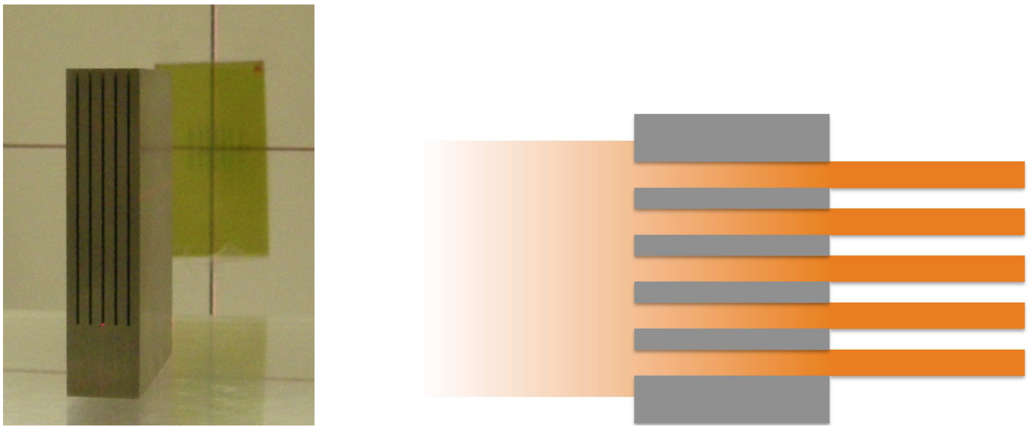

FIG. 1: On the left side is shown a photograph of the multislit collimator used to generate the oxygen and carbon minibeams. On the right, a scheme shows how the minibeams are generated by using the mechanical collimator (not to scale).

B. Dosimetry

One of the main aims of this work was to perform a first dosimetry study in carbon and oxygen MBRT. The task is very challenging and error prone due to the extremely small field sizes used. New physical aspects, such as the volume averaging effect [28] or the lack of secondary electron equilibrium [29], start to play a non-negligible role and the approximations of classical radiation physics tend to be valid to a lesser extend compared to larger fields.

In addition, LET dependence is a limiting factor concerning detector choice in particle therapy, with the exception of the ionization chambers. However, currently there is no available ionization chamber providing a sub-millimetric spatial resolution. For all the aforementioned reasons, in this work, two independent detector systems were used: *i)* the PTW microDiamond® single crystal diamond detector [30]; and *ii)* radiochromic films (EBT3) [31]. More details about these detectors are given later.

1. microDiamond® detector measurements

The PTW microDiamond® detector consists of a single crystal diamond detector (SCDD). It has a very small sensitive volume (0.004 mm^3) with a thickness of 1 μm in one of the directions, providing a micrometrical spatial resolution if used perpendicular to the measurement direction [30]. This makes the microDiamond® detector a very good candidate for small field dosimetry, as in the case of hadron MBRT. The performance of this type of detectors has already been proved in standard carbon therapy measurements [32]. In particular, it is one of the few existing detectors showing negligible LET dependence [32].

Measurements were performed in the MP3-P water tank phantom ($60\times60\times50$ cm^3) equipped with a 3-axis motor system [33]. The thickness of the PMMA entrance window of the water phantom was 3 mm (water equivalent path length of 3.5 mm). The detector was placed with the smallest thickness dimension (1 μm) perpendicular to the beam. The step size used for the measurements was 100 μm in steep dose gradient regions and was increased to 200 μm in low gradient dose regions. Profiles were measured at several depths in water (33, 53 and 83 mm). Direct measurements at shallower depths were not possible, due to the water tank wall and the space needed by the holder of the detector.

2. EBT3 film measurements

Measurements (twice per irradiation configuration) were also performed with EBT3 Gafchromic® films, which were placed perpendicularly to the incoming beam at different depths in a PMMA slab phantom. The positions of the films in the PMMA phantom were translated to water equivalent depth, by using a depth scaling factor (1.165) [34].

Radiochromic films provide the high spatial resolution required by the small field sizes used and they were already successfully used in x-ray and proton MBRT [19, 35–37]. Films were analyzed with a flat bed scanner (Epson Perfection V750-M Pro Scanner) at 1200 dpi, using the methodology described in the work of Devic *et al.* [38]. For the handling of the films, the recommendations provided by Task Group 55 of the American Association of Physics in Medicine (AAPM) [39] were taken into account. Following the work of Martišíková and Jäkel [40], a photon calibration (^{137}Cs, 662 keV photons) was performed. In addition, the triple channel method was used for film dosimetry.

A comparison between dose measurements with an ionization chamber (TM30013 PTW Farmer®, sensitive volume of 0.6 cm^3) and with the radiochromic films was performed at several depths with the classical seamless irradiation field, in order to evaluate quenching effects [40]. Figure 2 shows film sensitivity dependence as a function of depth for both detectors. Film sensitivity is reduced at depth, due to LET increase towards the end of the particle track. In the case of carbon beams, this reduction is around 20% at the center of the SOBP region. As expected, the corresponding values for oxygen (around 40%) are larger than for carbon beams. Dose values obtained with the films were corrected by quenching effects.

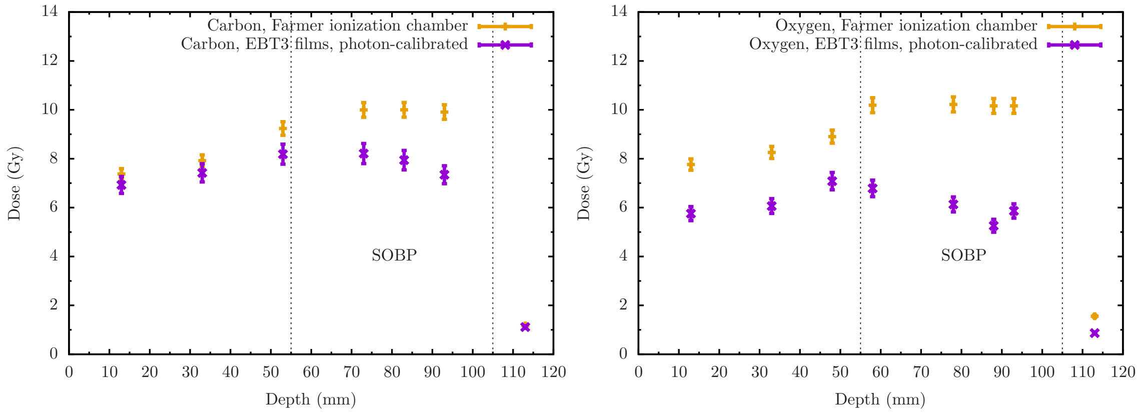

FIG. 2: Carbon (left) and oxygen (right) dose measurements at several depths in a solid water phantom. Doses were measured with the TM30013 PTW Farmer ionization chamber and with the EBT3 radiochromic films to evaluate quenching effects. The irradiation field size was 50×50 mm^2 (classical seamless irradiation field).

III. RESULTS AND DISCUSSION

This section reports on the dosimetric results obtained, which constitute the first experimental proof of feasibility of the technique and an evaluation of the detectors chosen. This dosimetry study could serve to guide the first biological experiments of this innovative approach. We mainly focused on the peak-to-valley dose ratio (PVDR), which is an essential dosimetric parameter in spatially fractionated techniques for its role in biological response [16]. Output factors (OF), penumbra values and the beam full width at half maximum (FWHM) were also assessed.

Figure 3 shows the lateral dose profiles for carbon and oxygen MBRT, showing the spatial fractionation of the dose. The observed reduction of PVDR values with lateral distance might arise from the use of 'large' focal spots (FWHM between 4 to 7 mm; see Table I), as well as from the initial collimator design. Further optimization of the collimator and/or beamline setup might lead to improved dose distributions.

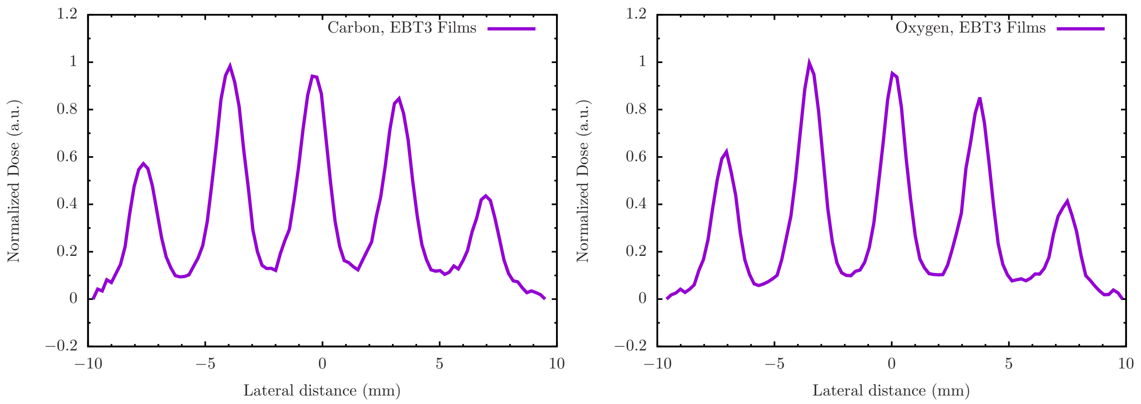

FIG. 3: Lateral dose profiles for carbon (left) and oxygen (right) MBRT measured with EBT3 radiochromic films are represented at 95.8 mm water equivalent depth. The irradiation field size was 15×15 mm^2.

Central PVDR values as a function of depth are presented in Figure 4 (on the left, for carbon MBRT and, on the right, for oxygen MBRT). As explained in section II B, due to the extreme irradiation conditions, two independent detector systems (microDiamond® detector and EBT3 Gafchromic® films) were used.

The two sets of measurements, displayed in Figure 4, are in good agreement. The PVDR values for both ions follow the same trend. The highest PVDR is found near the phantom surface, reaching a value of 50–60 at 10 mm-depth. Then, PVDR values decrease due to multiple Coulomb scattering and the contribution of secondary fragments in depth, that fill the valleys. Carbon minibeams present slightly lower PVDR values with respect to oxygen minibeams. However, in both cases, the PVDR values obtained in normal tissues are significantly higher than in x-rays MBRT [24], for which a net gain in tissue sparing has been shown [11]. This supports the potential of carbon and oxygen MBRT for normal tissue sparing capability. A quasi-homogeneous dose distribution or lower PVDR values may be obtained in the tumor by using interlaced irradiations, as in previous spatially fractionated RT techniques studies [41, 42].

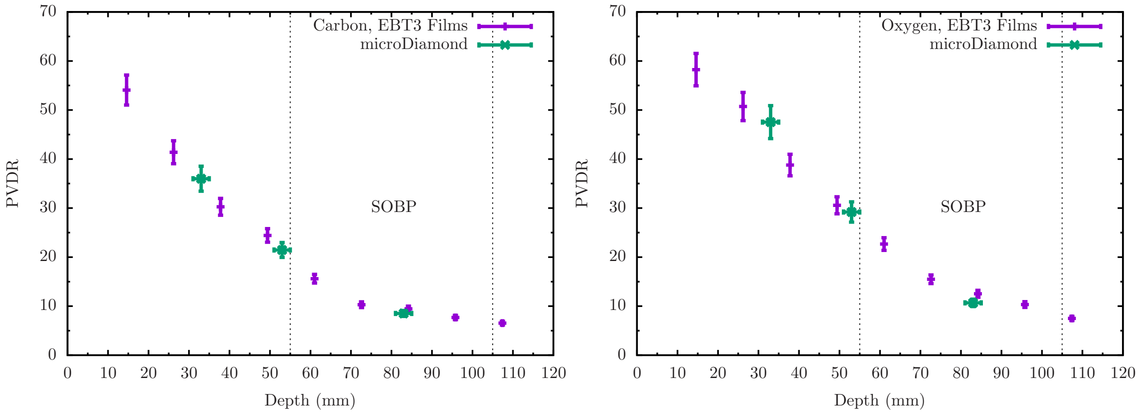

FIG. 4: Central PVDR values as a function of the water equivalent depth for carbon (left) and oxygen (right) MBRT measured with the microDiamond® detector and the EBT3 radiochromic films. The irradiation field size was 15×15 mm^2.

The FWHM of the central beam and the penumbra (measured as the lateral distance between 80% and 20% of the maximum dose) are represented in Figures 5 and 6, respectively. They were assessed from EBT3 radiochromic measurements, due to the larger spatial resolution with respect to the microDiamond® (limited to 100–200 μm).

Both FWHM and penumbra values increase as a function of depth, due to multiple Coulomb scattering. Central beam FWHM range between around 700–1700 μm and between 700–1500 μm for carbon and oxygen ions, respectively. These values are largely reduced with respect to pMBRT, where FWHM values range from 1000 μm at the entrance up to 2500 μm at 40 mm-depth [19].

In addition, penumbra values are extremely narrow (less than 1000 μm in the case of carbon beams, and less than 750 μm for oxygen beams) in comparison with the 3–5 mm penumbras in standard radiosurgery [43], which would benefit the sparing of delicate adjacent structures.

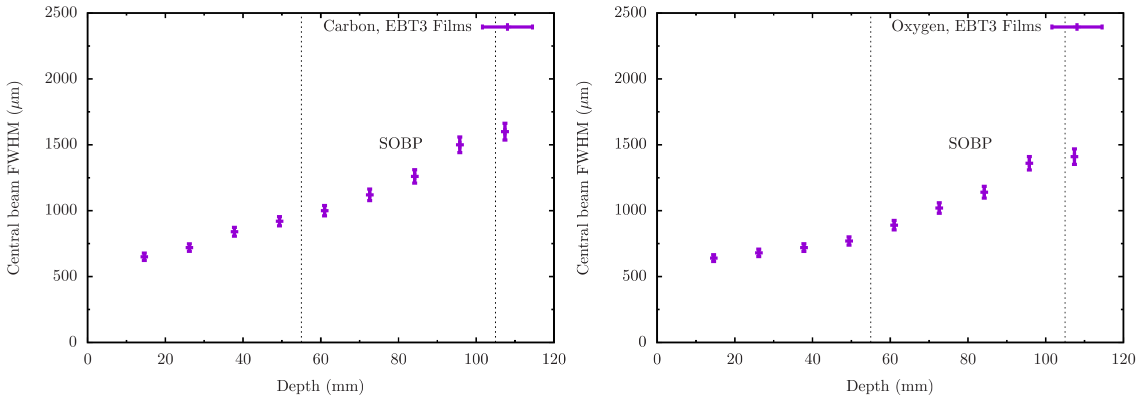

FIG. 5: Central beam FWHM as a function of the water equivalent depth for carbon (left) and oxygen (right) MBRT measured with EBT3 radiochromic films.

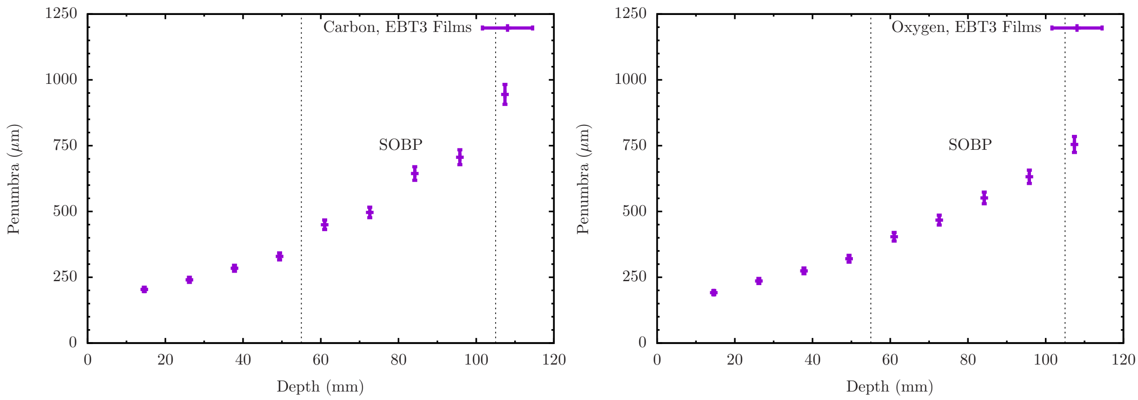

FIG. 6: Penumbra as a function of the water equivalent depth for carbon (left) and oxygen (right) MBRT measured with EBT3 radiochromic films.

Finally, OF were evaluated for carbon and oxygen beams at 83 mm-depth (center of SOBP region) as the central minibeam peak dose with respect to the corresponding dose in broad beam configuration for a field size of 15×15 mm^2. Due to the sub-millimetric field sizes used in this work, low OF values are obtained. In particular, for carbon beams, the OF are 0.37 ± 0.02 (EBT3 Gafchromic®) and 0.34 ± 0.02 (microDiamond®), respectively, showing a good agreement between both detectors. In the case of oxygen beams, the values are slightly higher (around 0.37 ± 0.03). Both values are higher than in proton MBRT, for which the OF was around 0.2 at 80 mm-depth [19] due to the reduced lateral scattering with respect to proton minibeams. Higher output factors might be obtained with an optimized beam application system (*i.e.* active collimation, as shown in [44]).

IV. CONCLUSION

This work presents an experimental dosimetric study in carbon and oxygen MBRT. It is the first time that measurements in sub-millimetric field sizes in carbon and oxygen therapy are reported. Two different detector systems (microDiamond® detector and EBT3 Gafchromic® films) were used. The two sets of measurements show a good agreement, confirming the reliability of those systems for small field dosimetry in mixed LET irradiations, when proper corrections are applied.

Moreover, the PVDR values measured (up to 60) are significantly higher than the ones obtained in x-rays MBRT, for which a net gain in tissue sparing has been proven. This suggests that carbon and oxygen MBRT might lead to a significant reduction of normal tissue complication probability. This benefit would be achieved in addition to the already existing advantages of hadron beams, *i.e.* their inverse dose profile and the enhanced biological effectiveness in the tumor.

The confirmation of the potential of this innovative approach requires the realization of biological experiments. If successful, this could open the door for a dose escalation in the tumor, of special interest in the case of radio-resistant tumors, like gliomas. Next steps include the further optimization of beamline setup and minibeam generation, including neutron background contamination assessment, as well as biological evaluations.

Acknowledgments

The authors warmly thank HIT and FP7 (Grant Agreement no 228436) for granting beam-time. We gratefully acknowledge the assistance of Udo Bauer and Lorena Magallanes. IMR has the support of the *Secretaria d'Universitats i Recerca del Departament d'Economia i Coneixement de la Generalitat de Catalunya* and of the European Union's Research and technological Innovation 7th framework program under the Marie Curie COFUND program (contract No. 600385).

There is no conflict of interest or financial disclosures statement to declare.

---

[1] R. R. Wilson, "Radiological use of fast protons", Radiology **47**, 487–491 (1946).

[2] G. Kraft, "Tumor therapy with heavy charged particles", Prog. Part. Nucl. Phys. **45**, S473–S544 (2000).

[3] D. Schardt, T. Elsässer and D. Schulz-Ertner, "Heavy-ion tumor therapy: Physical and radiobiological benefits", Rev. Mod. Phys. **82**, 383–425 (2010).

[4] B. L. Ramaekers, M. Pijls-Johannesma, M. A. Joore, P. van den Ende, J. A. Langendijk, P. Lambin, A. G. Kessels and J. P. Grutters, "Systematic review and meta-analysis of radiotherapy in various head and neck cancers: comparing photons, carbon-ions and protons", Cancer. Treat. Rev. **37**, 185–201 (2011).

[5] M. Lodge, M. Pijls-Johannesma, L. Stirk, A. J. Munro, D. De Ruysscher and T. Jefferson, "A systematic literature review of the clinical and cost-effectiveness of hadron therapy in cancer", Radiother. Oncol. **83**, 110–122 (2007).

[6] D. R. Olsen, O. S. Bruland, G. Frykholm and I. N. Norderhaug, "Proton therapy – A system-

atic review of clinical effectiveness", Radiother. Oncol. **83**, 123–132 (2007).

[7] Particle Therapy Co-Operative Group (PTCOG), `ptcog.web.psi.ch` (2013).

[8] T. Okada, T. Kamada, H. Tsuji, J. Mizoe, M. Baba, S. Kato, et al., "Carbon Ion Radiotherapy: Clinical Experiences at National Institute of Radiological Science (NIRS)", J. Radiat. Res., **51**, 355-364 (2010)

[9] F.A. Dilmanian,Z. Zhong, T. Bacarian, H. Benveniste, P. Romanelli, R. Wang, J. Welwart, T. Yuasa, E. M. Rosen and D.J. Anschela, "Interlaced x-ray microplanar beams: A radiosurgery approach with clinical potential", Proc. Natl. Acad. Sci. USA **103**, 9709–9714 (2006).

[10] P. Deman, M. Vautrin, M. Edouard, V. Stupar, L. Bobyk, R. Farion, H. Elleaume, C. Remy, E. L. Barbier, F. Esteve and J.F. Adam, "Monochromatic minibeams radiotherapy: From healthy tissue-sparing effect studies toward first experimental glioma bearing rats therapy", Int. J. Radiat. Oncol. Biol. Phys. **82**, e693–e700 (2012).

[11] Y. Prezado, P. Deman, P. Varlet, G. Jouvion, S. Gil, C. Le Clech, H. Bernard, G. Le Duc, S. Sarun, "Tolerance to dose escalation in minibeam radiation therapy applied to normal rat brain: long-term clinical, radiological and histopathological analysis", Radiat. Res. **184**, 314–321 (2015).

[12] C. Peucelle, I. Martínez-Rovira and Y. Prezado, "Spatial fractionation of the dose using neon and heavier ions: a Monte Carlo study", Med. Phys. **42**, 5928–5936 (2015).

[13] F. Tommasino, E. Scifoni and M. Durante, "New Ions for Therapy", Int. J. Part. Ther. **2**, 428–438 (2016).

[14] I. Martínez-Rovira and Y. Prezado, "Minibeam radiation therapy for the management of osteosarcomas: A Monte Carlo study", Med. Phys. **41**, 061706 (2014).

[15] I. Martínez-Rovira, G. Fois and Y. Prezado, "Dosimetric evaluation of new approaches in

GRID therapy using nonconventional radiation sources", Med. Phys. **42**, 685–693 (2015).

[16] F.A. Dilmanian, T.M. Button, G. Le Duc, N. Zhong, L.A. Pena, J.A. Smith, S.R. Martinez, T. Bacarian, J. Tammam, B. Ren, P.M. Farmer, J. Kalef-Ezra, P.L. Micca, M.M. Nawrocky, J.A. Niederer, F.P. Recksiek, A. Fuchs and E.M. Rosen, "Response of rat intracranial 9L gliosarcoma to microbeam radiation therapy", Neuro Oncol. **4**, 26–38 (2002).

[17] I. Martínez-Rovira, J. Sempau, J.M. Fernández-Varea, A. Bravin and Y. Prezado, "Monte Carlo dosimetry for forthcoming clinical trials in x-ray microbeam radiation therapy", Phys. Med. Biol. **55**, 4375–4388 (2010).

[18] Y. Prezado and G. Fois, "Proton-minibeam radiation therapy: a proof of concept", Med. Phys. **40**, 031712-1–8 (2013).

[19] C. Peucelle, C. Nauraye, A. Patriarca, E. Hierso, N. Fournier-Bidoz, I. Martínez-Rovira, and Y. Prezado, "Proton minibeam radiation therapy: Experimental dosimetry evaluation", Med. Phys. **42**, 7108–7113 (2015).

[20] F. A. Dilmanian, A. Rusek, G. R. Fois, J. Olschowka, N. R. Desnoyers, J. Y. Park, I. Dioszegi, B. Dane, R. Wang, D. Tomasi, H. Lee, S. D. Hurley, P. K. Coyle, A. G. Meek, M. K. O'Banion, "Interleaved carbon minibeams: an experimental radiosurgery method with clinical potential", Int. J. Radiat. Oncol. Biol. Phys. **84**, 514–519 (2012).

[21] Heidelberg Ion-Beam Therapy Center (HIT), `www.klinikum.uni-heidelberg.de/`.

[22] T. Haberer, J. Debus, H. Eickhoff, O. Jäkel, D. Schulz-Ertner and U. Weber, "The Heidelberg ion therapy center", Radiother. Oncol. **73**, S186–S189 (2004).

[23] B. P. Poncelet, V. J. Wedeen, R. M. Weisskoff and M. S. Cohen, "Brain parenchyma motion: measurement with cine echo-planar MR imaging", Radiology **185** 645–651 (1992).

[24] Y. Prezado, I. Martínez-Rovira, S. Thengumpallil and P. Deman, "Dosimetry protocol for

the preclinical trials in white-beam minibeam radiation therapy", Med. Phys. **38**, 5012–5020 (2011).

[25] M. Krämer, O. Jäkel, T. Haberer, G. Kraft, D. Achardt and U. Weber, "Treatment planning for heavy-ion radiotherapy: physical beam model and dose optimization", Phys. Med. Biol. **45**, 3299–3317 (2000).

[26] M. Krämer and M. Scholz, "Treatment planning for heavy-ion radiotherapy: calculation and optimization of biologically effective dose", Phys. Med. Biol. **45**, 3319–3330 (2000).

[27] K. Parodi, A. Mairani, S. Brons, B. G. Hasch, F. Sommerer, J. Naumann, O. Jäkel, T. Haberer and J. Debus, "Monte Carlo simulations to support start-up and treatment planning of scanned proton and carbon ion therapy at a synchrotron-based facility", Phys. Med. Biol. **57**, 3759–3784 (2012).

[28] O. A. Sauer and J. Wilbert, "Measurements of output factors for small photon beams", Med. Phys. **34**, 1983–1988 (2007).

[29] I. J. Das, G. X. Ding, and A. Ahnesjö, "Small fields: Nonequilibrium radiation dosimetry", Med. Phys. **35**, 206–215 (2008).

[30] microDiamond® PTW detector, `http://www.ptw.de/2732.html`

[31] EBT3 Gafchromic® Films, `http://www.ashland.com/`

[32] M. Marinelli, G. Prestopino, C. Verona, G. Verona-Rinati, M. Ciocca, A. Mirandola, A. Mairani, L. Raffaele, G. Magro, "Dosimetric characterization of a microDiamond detector in clinical scanned carbon ion beams", Med. Phys. **42**, 2085–2093 (2015).

[33] MP3-P PTW Phantom Tank, `http://www.ptw.de/mp3-p_phantom_tank00.html`

[34] R. Zhang, P. J. Taddei,M. M. Fitzek and W. D. Newhauser, "Water equivalent thickness values of materials used in beams of protons, helium, carbon and iron ions", Phys. Med. Biol.

55, 2481–2493 (2010).

[35] I. Martínez-Rovira, J. Sempau and Y. Prezado, “Development and commissioning of a Monte Carlo photon beam model for the forthcoming clinical trials in Microbeam Radiation Therapy”, Med. Phys. **39**, 119–131 (2012).

[36] I. Martínez-Rovira, J. Sempau and Y. Prezado, “Monte Carlo-based treatment planning system calculation engine for microbeam radiation therapy”, Med. Phys. **39**, 2829–2838 (2012).

[37] I. Martínez-Rovira, J. Sempau and Y. Prezado, “Monte Carlo-based dose calculation engine for minibeam radiation therapy”, Phys. Med. **30**, 57–62 (2014).

[38] S. Devic, J. Seuntjens, E. Sham, E. B. Podgorsak, C. R. Schmidtlein, A. S. Kirov and C. G. Soares, “Precise radiochromic film dosimetry using flat-bed document scanner”, Med. Phys. **32**, 2245–2253 (2005).

[39] A. Niroomand-Rad, C. R. Blackwell, B. M. Coursey, K. P. Gall, J. M. Galvin, W. L. McLaughlin, Al. S. Meigooni, R. Nath, J. E. Rodgers and C. G. Soares, “Radiochromic film dosimetry: Recommendations of AAPM Radiation Therapy Committee Task Group 55”, Med. Phys. **25**, 2093–2115 (1998).

[40] M. Martišíková and O. Jäkel, “Dosimetric properties of Gafchromic® EBT films in medical carbon beams”, Phys. Med. Biol. **55**, 5557–5567 (2010).

[41] Y. Prezado, S. Sarun, S. Gil, P. Deman, A. Bouchet and G. Le Duc, “Increase of lifespan for glioma-bearing rats by using minibeam radiation therapy”, J. Synchrotron Radiat. **19**, 60–65 (2012).

[42] B. Pouyatos, R. Serduc, M. Chipaux, T. Chabrol, E. Brauer-Krisch, C. Nemoz, H. Mathiew, O. David, L. Renaud, Y. Prezado, J.A. Laissue, F. Estève, S. Charpier and A. Depaulis, “Synchrotron X-ray interlaced microbeams suppress paroxysmal oscillations in neuronal networks

initiating generalized epilepsy", Neurobiology of Disease **51**, 152–160 (2013).

[43] M. Guerrero, X.A. Li and L. Ma, "A technique to sharpen the beam penumbra for Gamma Knife radiosurgery", Phys. Med. Biol. **21**, 1843–1853 (2003).

[44] C. Peucelle, Ph.D. Thesis "Spatial fractionation of the dose in charged particle therapy" (Université Paris-Saclay, November 2016).